Korean J. Chem. Eng., 33(7), 2063-2072 (2016)
DOI: 10.1007/s11814-016-0060-3

pISSN: 0256-1115
eISSN: 1975-7220

Transesterification of soybean oil to biodiesel by tin-based Brønsted-Lewis acidic ionic liquid catalysts

Xiaoxiang Han*,†, Wei Yan*, Chin-Te Hung, Yanfei He*, Pei-Hao Wu**, Li-Li Liu**, Shing-Jong Huang***, and Shang-Bin Liu**,†**

*Department of Applied Chemistry, Zhejiang Gongshang University, Hangzhou 310035, China
**Institute of Atomic and Molecular Sciences, Academic Sinica, Taipei 10617, Taiwan
***Instrumentation Center, National Taiwan University, Taipei 10617, Taiwan
(*Received 18 November 2015 • accepted 22 February 2016*)

Abstract−A series of Brønsted-Lewis acidic ionic liquid (BLAIL) catalysts consisting of sulfonated ionic liquid [SO_3H-pmim]Cl and Sn(II) chloride have been synthesized and exploited for catalytic transesterification of soybean oil with methanol to biodiesel. The structural and chemical properties of these [SO_3H-pmim]Cl-*x*$SnCl_2$ (x=0-0.8) catalysts were characterized by different analytical and spectroscopic techniques, such as FT-IR, TGA, and NMR. In particular, their acid properties were studied by solid-state ^{31}P NMR using trimethylphosphine oxide as the probe molecule. The BLAIL catalysts were found highly efficient for transesterification reaction due to the introduction of Lewis acidity by $SnCl_2$ in the initially Brønsted acidic [SO_3H-pmim]Cl catalyst. The effects of three independent process variables on biodiesel yield were optimized by response surface methodology (RSM). Consequently, an excellent biodiesel yield of 98.6% was achieved under optimized reaction conditions over the BLAIL catalyst with $SnCl_2$ loading (*x*) of 0.7.

Keywords: Brønsted-Lewis Acidic Ionic Liquid, Biomass, Transesterification, Biodiesel, Optimization, Response Surface Methodology

INTRODUCTION

In view of the serious shortage in energy resources and increasing concerns on environmental issues, R&D relevant to production of biodiesel has attracted considerable attention. Biofuels have been recognized as alternative economical and renewable energy that may be derived from various biomass feedstocks such as lignocellulose and triglycerides. In particular, biodiesel (i.e., fatty acid methyl esters; FAME) may be produced from catalytic conversion of triglycerides through esterification or transesterification reactions. Triglycerides are mixtures of glycerol and fatty acids with varied carbon chain lengths (C_{12}-C_{18}) and C=C bonds, which may be extracted from various waste feedstocks such as animal fats, vegetable oils, plant or seed oils, or waste oils. Compared to fossil fuels, biodiesel has low viscosity, biodegradability, high flash point, nontoxicity, low SO_x/CO emission, and feasibility in blending with fossil diesel and so on. Moreover, biodiesel can be directly applied in conventional diesel engines without further modifications [1].

In general, the synthesis of biodiesel invoking esterification or transesterification reaction inevitably requires an acid or base catalyst, which may either be homogeneous (liquids) or heterogeneous (organic or inorganic solids). For the latter, alkalines, mineral acids, ion-exchange resins, polymeric acids, metal oxides, zeolites, functionalized porous materials, and heteropolyacids are commonly used [2-10]. Although basic catalysts are also employed for esterification/transesterification reactions, the processes invoked are more rigorous (e.g., mass fraction of fatty acid should be no more than 0.5%), which largely limits its industrial applications. Nevertheless, conventional acidic catalysts may also be limited by activity, environmental safety, and process management issues. For example, some acid catalysts have drawbacks of weak acidity, active site inaccessibility, vulnerability to deactivation, mass transfer limitation, hazard waste treatment, difficult recovery and reuse, and so on. In this context, acidic ionic liquids (AILs) are regarded as alternative green catalysts owing to their unique properties, such as low vapor pressure, high thermal stability and solubility, adjustable physicochemical properties, tunable acidity, eco-friendliness and self-separation characteristics, and reusability [11]. Consequently, AILs have been widely used as efficient catalyst in chemical industries due to their fast reaction rate [12]. In particular, AILs possessing active Lewis [13,14] or Brønsted [15-21] acid sites have been exploited for the synthesis of biodiesel. More recently, AIL catalysts with coexisting Lewis and Brønsted acidities have been reported and showed prominent and perspective applications in polymerization, transesterification, and oxidation reactions [22-28]. Compared with purely Lewis or Brønsted AILs, the high catalytic activity observed for the BLAIL catalysts has been attributed to the synergy of Brønsted and Lewis acid sites [29].

We report herein a novel series Brønsted-Lewis acid ionic liquid (BLAIL) catalysts, which were synthesized by incorporating stannous chloride ($SnCl_2$, which served as the Lewis acid center) with a Brønsted acid-based propanesulfonate-functionalized methylimidazolium (MIM-PS) zwitterion ionic liquid. The acid properties of such BLAIL catalysts were characterized by ^{31}P NMR using tri-

†To whom correspondence should be addressed.
E-mail: hxx74@126.com, sbliu@sinica.edu.tw

methylphosphine oxide (TMPO) as the probe molecule [30-34]. Their catalytic activities during transesterification of soybean oil to biodiesel were investigated. Over the most efficient catalyst, relevant experimental conditions were optimized using response surface methodology (RSM) [35,36], and recyclability was also examined.

EXPERIMENTAL

1. Preparation of BLAILs

The BLAIL catalysts were synthesized by a modified procedure inspired by an earlier report [37]. In brief, an equimolar mixture of methylimidazole (0.1 mol, 8.2 g) and 1,3-propanesultone (0.1 mol, 12.2 g) was first dissolved in ethyl acetate (30 mL) while soaking in an ice bath followed by stirring at 323 K for 2 h. After solidification, the resultant zwitterion 3-(1-methylimidazolium-3-yl)propane-1-sulfonate (MIM-PS) product was washed with ethyl acetate for three times, then dried under a vacuum manifold. Subsequently, a stoichiometric amount of hydrochloric acid (HCl; 0.1 mol) was added to an aqueous solution of zwitterion MIM-PS precursor, followed by stirring at 363 K for 2 h. After a water removal treatment, the white viscous intermediate so obtained was subjected to washing with toluene to obtain 1-methy-3-(propane-3-sulfonate group) imidazolium hydrochloric acid (denoted as [HO_3S-pmim]Cl). To 1.0 mol of this intermediate, varied amounts of anhydrous stannous chloride ($SnCl_2$, 0.5-0.8 mol) were added in batches for 1 h. The mixture was allowed to stir at 363 K for 2 h, then, the white viscous liquid was dried under vacuum to obtain a series of supported $SnCl_2$ catalysts, denoted as [HO_3S-pmin]Cl-*x*$SnCl_2$, where x is the amount of $SnCl_2$ added (in mole). All other chemicals were classified as research purity grade and were used without further purification unless otherwise stated.

2. Catalyst Characterization

Fourier-transform infrared (FT-IR) spectra of various samples (packed in KBr) were recorded on a Nicolet 380 spectrometer. Thermogravimetric and differential thermogravimetric (TG-DTG) curves were obtained on a Mettler Toledo (DSC 1 STARe system) thermal analyzer. Typically, samples were heated from room temperature (298 K) to 873 K at a heating rate of 10 K/min under flowing air. The structural compositions of the catalyst samples (dissolved in D_2O) were confirmed by ^1H and ^{13}C NMR spectroscopy using a Bruker AV 500 spectrometer. Their acidic properties were probed by solid-state ^{31}P NMR of adsorbed TMPO [30-34]. The experiments were carried out on a Bruker-Biospin Avance III 300 spectrometer using a 4 mm double-resonance magic-angle-spinning (MAS) probehead at a Larmor frequency of 121.50 MHz. All free induction decay (FID) signals were acquired using a single-pulse sequence with a pulse length of 1.5 μs (π/6 pulse) and a recycle delay of 10 s while under a sample spinning rate of 12 kHz. The ^{31}P chemical shifts were referenced to aqueous 85% H_3PO_4 in D_2O. The TMPO probe molecule was loaded onto the catalyst sample following a standard operation procedure described elsewhere [29,33].

3. Catalytic Reaction

The catalytic activity of various [HO_3S-pmin]Cl-*x*$SnCl_2$ (*x*=0-0.8 mol) catalysts was assessed by transesterification reaction of soybean oil with methanol. Typically, the reaction was carried out by first mixing desirable amounts of soybean oil (normally fixed at 0.1 mol) with methanol (methanol/soybean oil ratio=20-35 mol/mol), together with varied amounts of the BLAIL catalyst (4-10 wt%) in a 100 mL stainless steel autoclave equipped with a magnetic stirrer and a thermometer. After the oil bath was stirred at different temperatures (393-433 K) for a desirable period of time (3-24 h), the reaction mixture was then cooled to room temperature by a water bath. One of the unique characteristics of such reaction system is that the reaction products and catalyst will self-separate automatically after the reaction mixture stands for a short period of time (typically for ca. 0.5 h), forming a biphasic liquid layer. The upper layer containing the biodiesel products and methanol may be separated easily, while the BLAIL catalysts in the bottom layer may be recycled after a simple purification (with ethyl acetate), washing (with toluene), and drying (at 373 K under vacuum; 5 h) treatment. Chemical analysis of the product was by gas chromatography (GC; Agilent 6890N) apparatus equipped with a frame ionization detector and an HP-5 capillary column or GC with mass spectrometry (GC-MS; Agilent 7890A-5975C). Reactants and products were identified by comparing with authentic samples using methyl laurate as the internal standard. The product yield was defined as the weight ratio of the biodiesel, namely fatty acid methyl esters (FAME) to the soybean oil consumed during the reaction.

4. Experimental Design and Mathematical Model

To optimize the experimental conditions for the production of biodiesel over the synthesized BLAIL catalysts, response surface methodology (RSM) [35,36] with a confidence level of 95% was exploited. A Box-Behnken experimental design (BBD) [29,38] was chosen to investigate the effects of three independent process variables, namely, reactant molar ratio (x_1), catalyst amount (x_2), and reaction temperature (x_3) on biodiesel yield, as specified in Table 1. On the basis of such 3^3 BBD, a total of 17 sets of experiments (including 12 factorial points and 5 centering points) were performed. The three variables were tested at three levels coded with a plus signs (+1; high value), zero (0; center value), or a minus signs (−1; low value), which may be obtained by the following equation:

$$x_i = \frac{X_i - X_0}{\Delta X_i} \quad (1)$$

where x_i, X_i, and X_0 (i=1-3) represent the coded, real, and center values of the independent variable, respectively, and ΔX_i=(variable at high level−variable at low level)/2, which denotes the step change value.

A second-order model equation given by RSM was used to predict the optimized reaction process, interactive interactions between experimental variables, and the biodiesel yield (Y), which are the responses of the experimental design. The quadratic equation may

Table 1. List of symbols and coded levels for corresponding experimental variables and ranges used in the experimental design

Variable (unit)	Symbol	Range and level		
		−1	0	1
Methanol/soybean oil ratio (mol/mol)	x_1	25	30	35
Amount of catalyst (wt%)	x_2	6	8	10
Reaction temperature (K)	x_3	413	423	433

be expressed as:

$$Y = \beta_0 + \sum_{i=1}^{k} \beta_i x_i + \sum_{i=1}^{k} \beta_{ii} x_i^2 + \sum_{j=1}^{k} \beta_{ij} x_i x_{ij} + \varepsilon \quad (2)$$

where Y is the predicted product yield, x_i and x_j are the coded levels of the independent variables, β_0, β_i, β_{ii}, and β_{ij} denote the regression coefficients for the offset, linear, quadratic, and interaction terms (between variables i and j), respectively, k is the total number of variables being optimized, and ε represents the random error. Design-Expert software (Version 6.0.5, Stat-Ease Inc., USA) was used to analyze the experimental data, to perform analysis of variance (ANOVA), and to estimate of the regression equation. Accordingly, the fitted Eq. (2) may further be expressed by response surface and contour plots so that the correlations between the response and experimental variables at various coded levels may readily be visualized to facilitate optimization of process conditions. In addition, the coefficient of determination (R^2) may be used to evaluate the accuracy and applicability of the multiple regression model, and the significance of its regression coefficient may also be checked by the F-value obtained.

RESULTS AND DISCUSSION

1. Catalysts Characterization

Fig. 1 displays the FT-IR spectra of various [HSO_3-pmim]Cl-$x$$SnCl_2$ catalysts loaded with varied amount of $SnCl_2$ (x=0-0.8 mol; see Table 2). In spite of some slight shift in peak positions and variations in peak intensities, all peaks appeared to retain the characteristics of Brønsted acidic ionic liquid (AIL) observed for the pristine ILa ([HSO_3-pmim]Cl) catalyst [38]. The band at 3,398 and 2,928 cm^{-1} may be attributed to -OH vibrations and asymmetric stretching vibrations of -CH_2, respectively. The bands at 1,463 and 786 cm^{-1} may be assigned to bending and rocking vibrations of -CH_3, while those at 1,638 and 1,578 cm^{-1} should due to stretching vibrations of C=C and C=N bonds on the imidazole ring, respectively. On the other hand, the strong absorption bonds at 1,172 and 1,040 cm^{-1} should be associated with the asymmetric and symmetric stretching vibrations of S=O, respectively. Whereas, the catalysts also exhibited featured bands for organic groups, for example,

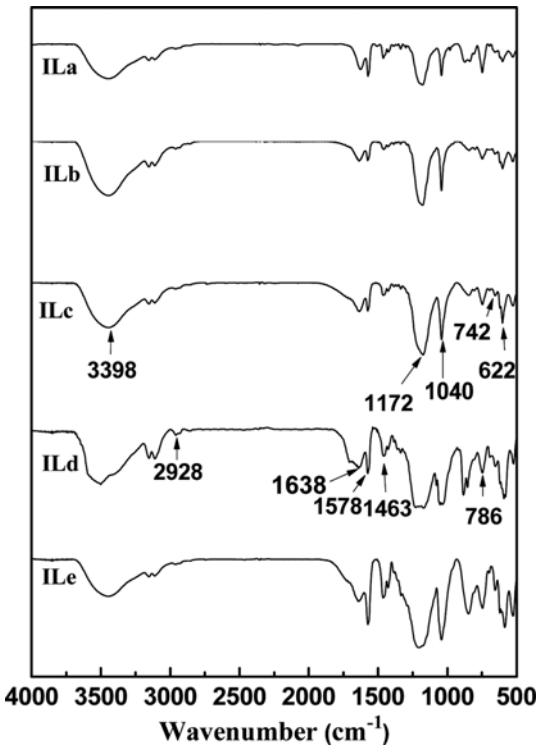

Fig. 1. FT-IR spectra of various AIL catalysts: ILa=[HSO_3-pmim]Cl; ILb=[HSO_3-pmim]Cl-0.5$SnCl_2$; ILc=[HSO_3-pmim]Cl-0.6$SnCl_2$; ILd=[HSO_3-pmim]Cl-0.7$SnCl_2$; ILe=[HSO_3-pmim]Cl-0.8$SnCl_2$.

the band at 742 cm^{-1} may be ascribed due to bending vibrations of the C-Cl bond.

Additional NMR measurements were also performed to further verify the structural integrity of various samples. Similar ^1H and ^{13}C NMR spectra were, respectively, observed for various [HO_3S-pmin]Cl-$x$$SnCl_2$ catalysts, indicating close resemblance of their structural compositions. As an illustration, the spectral data of the [HO_3S-pmin]Cl-0.7$SnCl_2$ (*i.e.*, ILd) catalyst are summarized below: ^1H NMR (500 MHz, D_2O); δ 2.207 (t, 2H), 2.813 (t, 2H), 3.784 (s, 3H), 4.254 (t, 2H), 7.338 (s, 1H), 7.411 (s, 1H), 8.643 (s, 1H) ppm; ^{13}C NMR (500 MHz, D_2O); δ 25.04, 35.68, 47.18, 47.70, 122.16, 123.74,

Table 2. Catalytic performance of various catalysts during transesterification of soybean oil with methanol

Catalyst[a]	Abbreviation	Appearance	Biodiesel yield (%)[c]
$SnCl_2$	---	Solid	56.6
[HO_3S-pmim]Cl	ILa	Liquid	75.3
[HO_3S-pmim]Cl-0.5$SnCl_2$	ILb	Liquid	80.3
[HO_3S-pmim]Cl-0.6$SnCl_2$	ILc	Liquid	90.1
[HO_3S-pmim]Cl-0.7$SnCl_2$	ILd	Liquid	98.4
[HO_3S-pmim]Cl+0.7$SnCl_2$[b]	ILd*	Liquid+solid	84.4
[HO_3S-pmim]Cl-0.8$SnCl_2$	ILe	Liquid+solid	94.9

[a]Various [HO_3S-pmim]Cl-$x$$SnCl_2$ (x=0-0.8) catalysts were prepared by adding x mol of $SnCl_2$ into 1.0 mol of [HO_3S-pmim]Cl intermediate, followed by stirring at 363 K for 2 h before drying

[b]Sample prepared by mixing 0.7 mol of $SnCl_2$ with 1.0 mol of [HO_3S-pmim]Cl at room temperature and was directly used without further stirring treatment at high temperature

[c]Reaction conditions: methanol/soybean oil=30 mol/mol, reaction time=24 h, reaction temperature=423 K, and catalyst amount=8 wt%

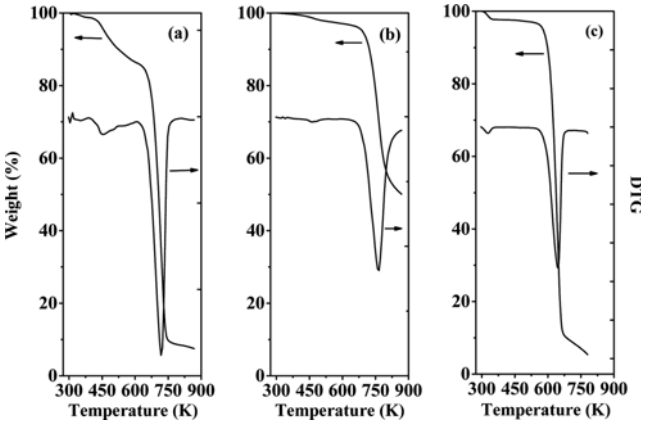

Fig. 2. TG-DTG curves of (a) [MIM-PSH]Cl, (b) [HSO_3-pmim]Cl-0.7$SnCl_2$, and (c) MIM-PS samples.

136.14 ppm. Moreover, the thermal stability of these BLAIL catalysts was examined by TGA-DTG analyses. Again, since similar TG-DTG profiles were observed for most BLAIL catalysts over the temperature range from room temperature to 873 K, only assorted results obtained from the zwitterionic MIM-PS precursor and Brønsted acidic [HO_3S-pmin]Cl (*i.e.*, ILa; Table 2) and Brønsted-Lewis acidic [HO_3S-pmin]Cl-0.7$SnCl_2$ (ILd; Table 2) IL catalysts are illustrated and discussed.

The pristine MIM-PS exhibited an initial weight-loss at ca. 340 K due to desorption of physisorbed water. In addition, the onset and final weight-loss were also observed at 550 and 684 K, respectively, with a corresponding DTG peak at 643 K (Fig. 2(a)) due to decomposition of the precursor. Whilst after the sulfonation treatment, the Brønsted acidic [HO_3S-pmin]Cl (ILa) intermediate showed the anticipated higher onset and final decomposition temperature of 610 and 776 K, respectively; corresponding to a DTG peak temperature of 720 K (Fig. 2(b)). Upon incorporation of Lewis active centers (i.e., $SnCl_2$), weight-losses occurring at even higher temperatures (463 and 773 K; Fig. 2(c)) were observed for the BLAIL catalyst (i.e., ILd=[HSO_3-pmim]Cl-0.7$SnCl_2$) gave an even higher onset (644 K) and final (>873 K) with a DTG peak at 765 K. Accordingly, the DTG peaks at 720 and 765 K observed for the latter two catalysts were attributed to the decomposition of the organic MIM-PS. These results indicate the successful anchoring of the anhydrous stannous chloride onto the intermediate and the ILd catalyst remain thermally stable at the reaction temperatures (393-433 K) adopted for the catalytic studies.

The acid properties of various samples were studied by solid-state ^{31}P MAS NMR of adsorbed trimethylphosphine oxide (TMPO) as the probe molecule. The ^{31}P-TMPO NMR approach has been demonstrated to be a powerful technique for acidity characterization not only solid [30-34] but also liquid [29,39,40] catalysts. More importantly, such approach is capable of probing acidic catalysts over a wide range of acidic strengths from weak, strong, to superacidic. The basic TMPO probe molecule tends to interact with the protic (Brønsted) acid sites, leading to the formation of $TMPOH^+$ ionic complexes, hence a down-field shift in the observed ^{31}P NMR chemical shifts (CSs), typically within the range of 50 to 95 ppm [31,33]. A higher observed ^{31}P CS value of the adsorbed TMPO

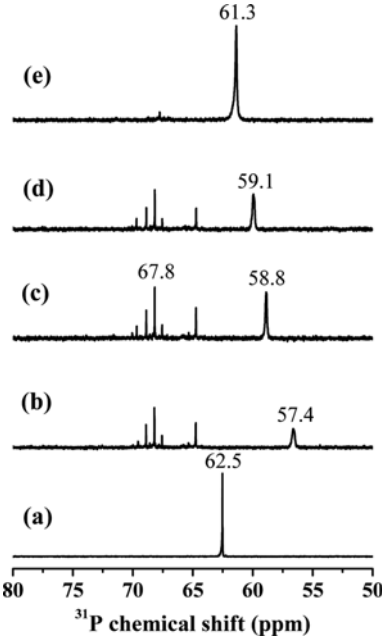

Fig. 3. ^{31}P NMR spectra of various AIL catalysts and (e) pure $SnCl_2$: (a) ILa=[HSO_3-pmim]Cl; (b) ILb=[HSO_3-pmim]Cl-0.5$SnCl_2$; (c) ILc=[HSO_3-pmim]Cl-0.6$SnCl_2$; (d) ILd=[HSO_3-pmim]Cl-0.7$SnCl_2$.

would correspond to Brønsted acid sites with a stronger acidic strength. In fact, a linear correlation between the observed TMPO chemical shift and Brønsted acidic strength may readily be inferred [30-34,39,40]. Fig. 3 shows the ^{31}P MAS NMR spectra of TMPO adsorbed on bulk $SnCl_2$ and various [HO_3S-pmin]Cl-*x*$SnCl_2$ (x= 0-0.7) AIL samples. All spectra were recorded on samples loaded with the same amount of TMPO guest molecule. The Brønsted acidic [HO_3S-pmin]Cl (*i.e.*, ILa) catalyst exhibited a sharp ^{31}P resonance at 62.5 ppm (Fig. 3(a)), a CS value much smaller than that observed for its sulfonated counterpart, [HO_3S-pmin]HSO_4, which revealed a CS value of 86.2 ppm [29] near the threshold of superacidity [33,39]. Upon incorporating $SnCl_2$ as Lewis acid centers, ^{31}P spectra of the Brønsted-Lewis acidic IL [HO_3S-pmin]Cl-*x*$SnCl_2$ catalysts showed multiple resonances, which may be categorized into two regions: region I (64-70 ppm) and region II (56-63 ppm). The ^{31}P resonances in region I may be attributed to the presence of $(TMPO)_2H^+$ adducts, *i.e.*, the absorption of two TMPO molecules per protic site [41]. These signals are irrelevant to the variations of ^{31}P CS with acidic strength discussed herein. Whereas, the ^{31}P signal in region II should arise from the anticipated $(TMPO)H^+$ complex. Moreover, the [HO_3S-pmin]Cl- *x*$SnCl_2$ BLAILs with x= 0.5, 0.6, and 0.7 (*i.e.*, ILb, ILc, and ILd catalysts; see Table 2) gave rise to a singlet peak at 57.4, 58.8, and 59.1 ppm, respectively (Figs. 3(b)-3(d)), approaching the CS value of 61.3 ppm observed for the Lewis acidic $SnCl_2$ (Fig. 3(e)). The above results indicate that all catalysts examined herein have only moderate acidity comparable to typical zeolitic catalysts (typically exhibit ^{31}P-TMPO CSs within 50-80 ppm) [30-34]. The abrupt decrease in the ^{31}P CS observed for the ILb catalyst upon introducing the $SnCl_2$ onto the purely Brønsted acidic ILa sample indicates a subtle balance between Brøn-

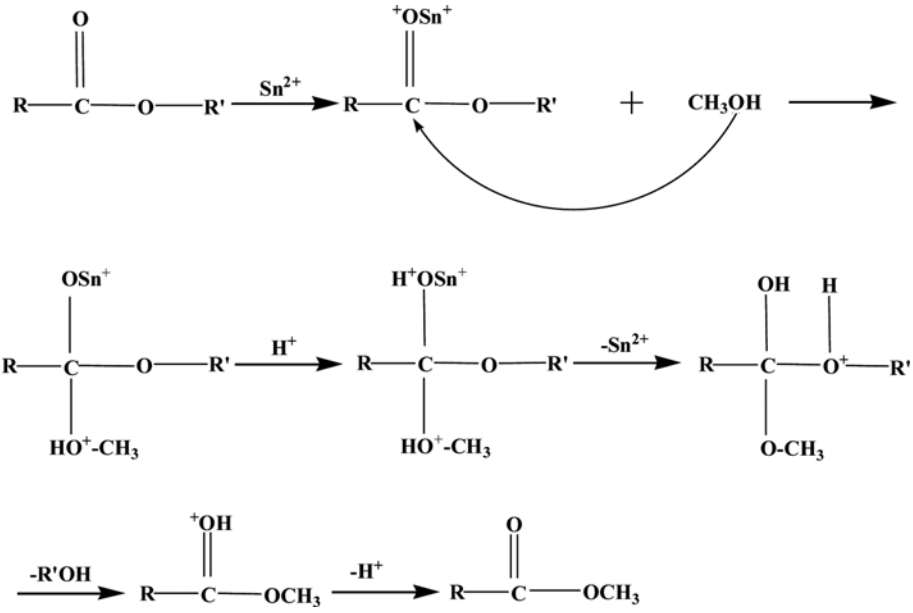

Scheme 1. Proposed mechanism for transesterification of soybean oil with methanol over the [HSO_3-pmim]Cl-*x*$SnCl_2$ (x=0.5-0.8) BLAIL catalyst.

sted and Lewis acidity. This is also supported by the gradual increase in ^{31}P-TMPO CS and peak intensity associated with the [HO_3S-pmin]Cl-*x*$SnCl_2$ BLAIL catalysts with increasing dosage of $SnCl_2$.

2. Transesterification of Soybean Oil with Methanol

The catalytic activity of the BLAIL catalysts was assessed by transesterification reaction of soybean oil with methanol. Their catalytic performance is depicted in Table 2. Note that the solid $SnCl_2$ catalyst, which has only Lewis acidity, exhibited only a biodiesel yield of only 56.6%. Likewise, the ILa ([HSO_3-pmim]Cl) catalyst, which has only Brønsted acidity, gave rise to a modest product yield of 75.3%. On the other hand, the [HSO_3-pmim]Cl-*x*$SnCl_2$ (0.5≤x≤0.8) catalysts showed enhanced activity with increasing x (*i.e.*, $SnCl_2$ loading), reaching a maximum biodiesel yield of 98.4% over the ILd catalyst (x=0.7). By comparison, a much lower biodiesel yield of 84.4% was observed over the [HO_3S-pmim]Cl+ 0.7$SnCl_2$ (denoted as ILd* in Table 2) sample prepared by physical mixing of mixing of $SnCl_2$ (0.7 mol) with [HO_3S-pmim]Cl (1.0 mol) at room temperature. However, further increasing the $SnCl_2$ loading (x≥0.8) in the BLAIL catalyst resulted in inferior catalytic performance. This is most likely due to diminishing of Brønsted acid sites in the presence of excessive Lewis acidity and the decrease in transport diffusivity of reactants and product. The above results are consistent with the increases in Lewis acidity and viscosity of the catalyst with increasing x. The afore-discussed results on acidity by means of the ^{31}P-TMPO NMR approach indeed revealed that, upon incorporating $SnCl_2$ onto the ILa catalyst, the concurrent existence of Brønsted and Lewis acidity was observed for the [HSO_3-pmim]Cl-*x*$SnCl_2$ (0.5≤x≤0.8) series catalysts. Moreover, the amount of Lewis acidity tends to increase with increasing x (i.e., $SnCl_2$ loading) [42,43].

Thus, while transesterification of soybean oil requires only catalyst with modest acidic strength, the co-existence of Brønsted and Lewis acidities is also indispensable to ensuring enhanced activity. Accordingly, a possible catalytic mechanism is proposed, as shown in Scheme 1. In brief, the Sn^{2+} presence in the catalyst system tends to bond with the carbonyl oxygen (which exhibited strong electronegativity) of the soybean oil (which contains mostly unsaturated fatty acids) to form intermediate complexes, which provokes effective interactions between the carbonyl carbon and the oxygen atom of the methanol. Meanwhile, the presence of Brønsted acidic proton (H^+) may couple with the carbonyl oxygen, leading to lowering of charge negativity, hence, favoring the release of Sn^{2+} [37] and subsequently formation of biodiesel.

To explore the effects of key experimental parameters, such as amounts of reactants and catalyst, reaction temperature and duration, on catalytic performance of the BLAILs, the [HO_3S-pmim]Cl-0.7$SnCl_2$ (ILd) catalyst was used for further optimization studies. Note that while each experimental variable was varied, other parameters were kept constant at their predicted optimal values: methanol/soybean oil=30.5 mol/mol, reaction temperature=425 K, and catalyst amount=8.5 wt%, and reaction time=24 h, Moreover, because transesterification is a reversible reaction, an excessive amount of methanol was exploited to ensure a forward reaction to favor an effective biodiesel yield. Along this line, the effect of methanol to soybean oil molar ratio (i.e., variable x_1; Table 1) on biodiesel yield was studied, as shown in Fig. 4(a). A gradual increase in biodiesel yield with increasing methanol/soybean oil ratio was observed, reaching an optimal yield of 98% at a reactant ratio of 30 mol/mol, then, gradually declining with increasing ratio (Fig. 4(a)). The presence of excessive methanol not only shifted the equilibrium towards the production of biodiesel but also was an efficient solvent for the BLAIL catalyst. However, further increasing the methanol/oil molar ratio may lead to over dilution of the catalyst to render the occurrence of undesirable reverse reaction.

Similar trend can be inferred for the effect of catalyst amount on biodiesel yield, of which a maximum of 98.4% was observed

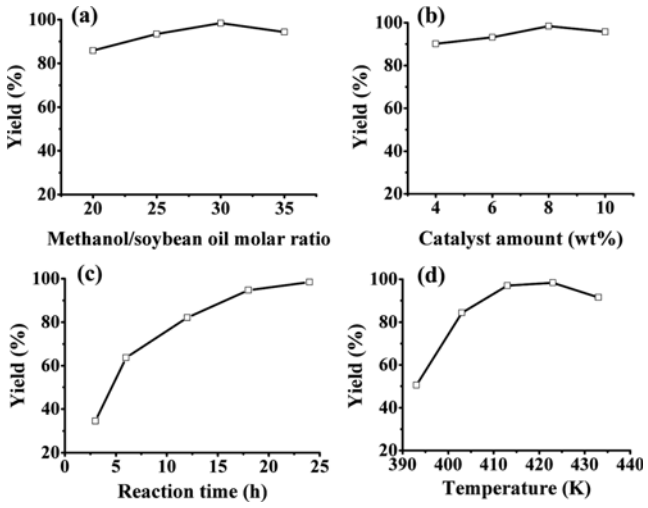

Fig. 4. Effects of (a) reactant molar ratio, (b) catalyst amount, (c) reaction time, and (d) reaction temperature on biodiesel yield during transesterification of methanol with soybean oil over the [HSO_3-pmim]Cl-0.7$SnCl_2$ AIL catalyst.

with 8 wt% of the [HO_3S-pmim]Cl- 0.7$SnCl_2$ catalyst (Fig. 4(b)). As the amount of BLAIL catalyst exceeded 8 wt%, the decline in biodiesel yield may have been due to the inevitable occurrence of side reaction provoked by enhanced acidity of the reaction system. Moreover, an anticipated increase in biodiesel yield with increasing reaction time was observed, reaching nearly 100% yield over a period of 24 h (Fig. 4(c)). The effect of reaction temperature on product yield was also examined, revealing a downward parabolic dependence with an optimal yield of 98.4% at 423 K (Fig. 4(d)). While, a higher reaction temperature is more favorable for the enhancement of reaction rate, and hence conversion efficiency. However, as the temperature exceeded 423 K, a notable increase in methanol vapor pressure occurred, which is undesirable for reversible exothermic reaction, leading to a descended catalytic activity and production yield.

Table 3. List of experimental design and response values

Entry	Variable and level[a]			Biodiesel yield (%)	
	x_1 (mol/mol)	x_2 (wt%)	x_3 (K)	Experimental	Calculated
1	1	1	0	94.7	94.6
2	1	−1	0	92.5	93.0
3	1	0	1	93.8	93.1
4	1	0	−1	92.1	92.4
5	−1	0	1	93.6	93.3
6	−1	0	−1	86.9	87.6
7	−1	1	0	93.6	93.1
8	−1	−1	0	89.8	89.9
9	0	1	1	94.8	95.6
10	0	1	−1	93.1	92.9
11	0	−1	1	93.6	93.8
12	0	−1	−1	90.7	89.9
13	0	0	0	98.3	98.3
14	0	0	0	98.6	98.3
15	0	0	0	97.8	98.3
16	0	0	0	98.1	98.3
17	0	0	0	98.8	98.3

[a]Variables and levels referring to Table 1: x_1=methanol/soybean oil molar ratio; x_2=catalyst amount; x_3=reaction temperature

3. Process Optimization

A factorial experimental design was used to optimize relevant experimental variables. The design of experiments, experimental results, and predicted responses for transesterification of soybean oil with methanol over the [HSO_3-pmim]Cl-0.7$SnCl_2$ AIL catalyst are depicted in Table 3. A total of 17 experimental runs was enforced.

Table 4. Estimated regression coefficients and corresponding statistical *F*- and *P*-values for biodiesel yield

Source	SOS[a]	DF[b]	Mean square	*F*-value	*P*-value	Significance[c]
Model	177.27	9	19.70	39.70	<0.0001	**
x_1	10.58	1	10.58	21.32	0.0024	**
x_2	11.52	1	11.52	23.22	0.0019	**
x_3	21.12	1	21.12	42.58	0.0003	**
x_1^2	53.36	1	53.36	107.55	<0.0001	**
x_2^2	18.75	1	18.75	37.78	0.0005	**
x_3^2	42.04	1	42.04	84.74	<0.0001	**
x_1x_2	0.64	1	0.46	1.29	0.2934	
x_1x_3	6.25	1	6.25	12.60	0.0094	**
x_2x_3	0.36	1	0.36	0.73	0.4225	
Residual	3.47	7	0.50			
Lack of fit	2.85	3	0.95	6.04	0.0575	
Pure error	0.63	4	0.16			
Cor. total	180.74	16				

[a]SOS=sum of squares
[b]DF=degree of freedom
[c]Symbol ** represents highly significant

The biodiesel yield (Y) may be correlated with independent experimental variables by a quadratic model, which can be expressed as:

$$Y=+98.32+1.15x_1+1.20x_2+1.62x_3-3.56x_1^2-2.11x_2^2-3.16x_3^2 -0.40x_1x_2-1.25x_1x_3-0.30x_2x_3 \quad (3)$$

where x_1, x_2, and x_3 are the coded values representing the three independent experimental variables, namely, methanol/soybean oil molar ratio, catalyst amount, and reaction temperature, respectively (*cf.* Table 1). From Eq. (3), it is indicative that the positive signs in front of the terms associated with x_1, x_2, and x_3 show that these variables have synergistic effect on the response, while other quadratic (interactive) terms, which have opposite signs, give rise to negative effects. Moreover, a close match between the experimental results and predicted response was observed.

To verify the fitting quality of the quadratic model in Eq. (3), statistical analysis based on the analysis of variance (ANOVA) was performed, as presented in Table 4. The observed model *F*-value (39.70) was much greater than its tabular counterpart (3.70), implying that the model was indeed significant. In addition, the obtained *P*-value (<0.0001) revealed that the chance (0.01%) that such a large 'model *F*-value' could occur was close to noise level. The small observed "Lack of Fit" *P*-value (Prob>F) of 0.0575 implies that the model fit the data well and was significant. A coefficient of determination (R^2=0.9808) was attained, indicating that the model was reliable in predicting the response. The "Adeq Precision" (19.890), which represents a measure of the signal to noise ratio, was also much greater than the desirable value of 4, as expected. Moreover, the relatively low observed coefficient of variation (0.75%) also demonstrated a high precision of the model and the experiments were reproducible. Based on these statistical test results, it is con-

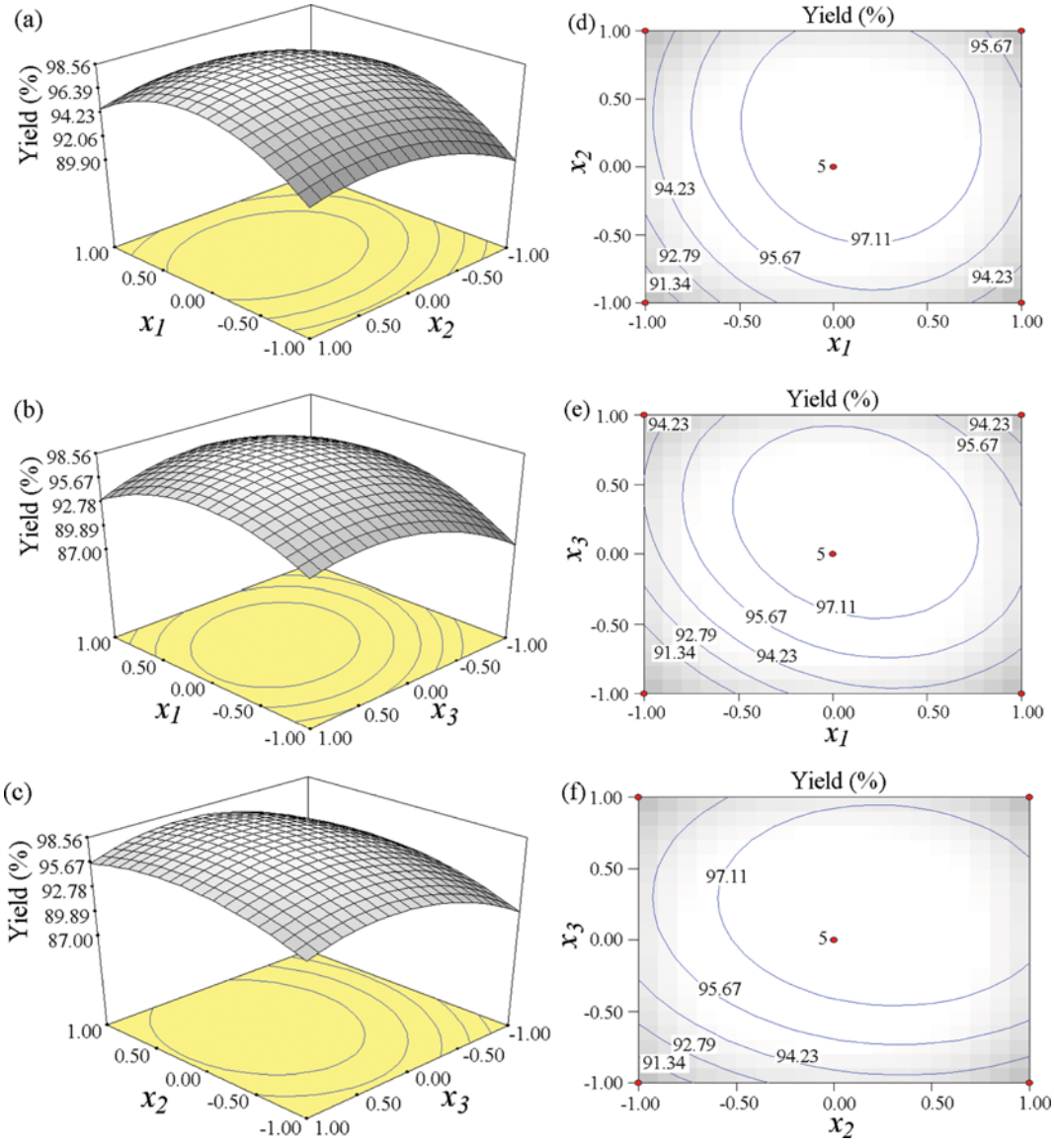

Fig. 5. (a)-(c) 3D response surface and (d)-(f) contour plots showing variations between a pair of experimental variables (Table 1) on the predicted values of biodiesel yield while keeping other variable at a constant level of 0: (a) and (d) methanol/oil ratio vs catalyst amount, (b) and (e) methanol/oil ratio vs reaction temperature, (c) and (f) catalyst amount vs reaction temperature.

clusive that the quadratic model is adequate for predicting a reliable biodiesel yield within the range of variables studied. This is supported by the observed *F*- and *P*-values, which revealed that all three independent variables and quadratic terms were highly significant to the predicted response.

The three-dimensional (3D) response surface and contour plots obtained from the predicted model are shown in Fig. 5. The correlations between the methanol/soybean oil molar ratio (x_1; Table 1) and the catalyst amount (x_2) at a fixed reaction temperature (x_3) and time are shown in Fig. 5(a). It can be seen that the biodiesel yield increased gradually to a maximum at relative low amount of catalyst, then, gradually decreased with increasing methanol/oil molar ratio, likely due to mass transfer limitation and excessive dilution of the catalyst. It is indicative that the methanol/oil molar ratio and catalyst amount have comparable effect on biodiesel yield during the transesterification reaction. This notion is consistent with the ANOVA results in Table 4 and the symmetrical mound shape contour lines in Fig. 5(d).

Figs. 5(b) and 5(e) show the interactive effects between methanol/oil molar ratio and reaction temperature on biodiesel yield. Upon increasing the reaction temperature, the biodiesel yield increased accordingly; however, as the temperature exceeded ca. 423 K, a decline in product yield due to rapid increase in vapor pressure of methanol was observed. On the other hand, a relatively weaker influence of biodiesel yield with methanol/oil molar ratio is evident. This is supported by the elliptical mound shape observed for the contour plot (Fig. 5(e)) and the ANOVA results in Table 4, which revealed that interaction of these two variables was significant. Similar conclusions may also be drawn for the interactive effect between the catalyst amount and reaction (Figs. 5(c) and 5(f)). The latter clearly has relatively more significant influence on biodiesel yield than the former, in good agreement with the ANOVA results (Table 4).

Based on the 17 sets of experimental data, optimized process conditions for the transesterification reaction may be derived as: x_1 (methanol/soybean oil ratio)=30.54 mol/mol, x_2 (catalyst amount)=8.52 wt%, and x_3 (reaction temperature)=425.24 K, corresponding to an optimal predicted biodiesel yield of 98.8%. To further confirm the reliability of the model fitting, three parallel experiments were carried out over the [HSO_3-pmim]Cl-0.7$SnCl_2$ BLAIL catalyst under the following realistic conditions: x_1=31 mol/mol, x_2=8.5 wt%, and x_3=425 K, leading to an average biodiesel yield of 98.6%, in close agreement to the above predicted value.

4. Compositions of Biodiesel

The biodiesel so produced during transesterification of soybean oil with methanol over the [HSO_3-pmim]Cl-0.7$SnCl_2$ BLAIL catalyst under the above optimized experimental conditions was analyzed by GC-MS using helium as the carrier gas under a flow rate of 1.0 mL/min. As a result, the peak assignments were accomplished based on their retention times, and a total biodiesel content of 98.2 wt% was achieved through normalization of peak areas. Among them, the concentration of saturated and unsaturated FAME (fatty acid methyl ester) was determined to be 46.0 and 53.2 wt%, respectively, including primary compounds such as methyl palmitate (34.8 wt%), methyl linoleate (44.4 wt%), and relatively small quantities of oleic acid methyl ester, stearic acid methyl ester, eicosanoic acid methyl ester, and docosanoic acid methyl ester.

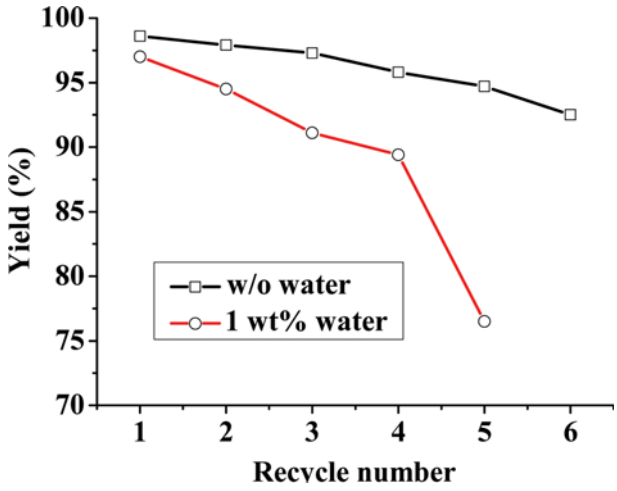

Fig. 6. Comparisons of durability of the [HSO_3-pmim]Cl-0.7$SnCl_2$ AIL catalyst during transesterification of soybean oil with methanol when with and without the presence of water. Reaction conditions: methanol/soybean oil molar ratio=31, catalyst amount=8.5 wt%, reaction temperature=425 K, and reaction time=24 h.

5. Recyclability of the BLAIL Catalyst

To assess the durability and recyclability of the BLAIL catalyst, the [HO_3S-pmim]Cl-0.7$SnCl_2$ sample was exploited for the recycling experiments. After each run, the BLAIL catalyst was purified with ethyl acetate, washing with toluene, then, dried under vacuum for 5 h at 373 K before reuse. Fig. 6 displays the variations of biodiesel yield after 5-6 consecutive runs without and with the presence of water, each carried out under the same reaction conditions: methanol/soybean oil ratio=31 mol/mol, catalyst amount=8.5 wt%, reaction temperature=425 K, and reaction time=24 h. In the absence of water, the [HO_3S-pmim]Cl-0.7$SnCl_2$ catalyst showed good durability for recycling use; the biodiesel yield decreased from 98.3 to 94.6% after six consecutive runs, which may be ascribed to slight deactivation of the AIL catalyst. Nevertheless, the catalyst exhibited an inferior stability when the transesterification reaction was carried out in the presence of small amount of water [44]; a biodiesel yield of 97.0% was obtained when 1 wt% of H_2O was introduced into the reaction system. In this case, although the reaction system sustained a reasonable biodiesel yield after three repeated cycles, the yield decreased notably to 76.3% when reaching the fifth cycle. As such, it is conclusive that the BLAIL catalysts reported herein, though exhibiting superior catalytic activity for transesterification of soybean oil, they are rather sensitive to water, hence, more preferable to be used under anhydrous condition.

CONCLUSIONS

A new series of acidic ionic liquid (AIL) catalysts have been successfully synthesized by coupling SO_3H-functionalized zwitterion ionic liquid with stannous chloride. These AIL catalysts, which possess both Brønsted and Lewis acidity with modest acidic strength, were found to be highly efficient for transesterification of soybean

oil with methanol. The synergy of Lewis and Brønsted acidity manifested catalytic activity during formation of biodiesel over these BLAIL catalysts. Over the [HSO_3-pmim]Cl-0.7$SnCl_2$ catalyst, a satisfactory biodiesel yield of 98.6% was achieved under optimized reaction conditions: methanol/oil ratio of 31, catalyst amount of 8.5 wt%, reactant temperature of 425 K, and reaction time of 24 h. In addition, the BLAIL catalysts reported herein also show unique self-separation characteristics to render facile product separation and catalyst recovery, and hence may have perspective applications in biofuel and chemical industries.

ACKNOWLEDGEMENTS

The support for this work by National Natural Science Foundation of China (No. 21177110), National Natural Science Foundation of Zhejiang province, China (No. LY13B070005), the Program for Zhejiang Leading Team of S & T Innovation (No. 2013TD07) and Ministry of Science and Technology, Taiwan (MOST104-2113-M-001-019) is gratefully acknowledged.

LIST OF NOMENCLATURE

AIL	: acidic ionic liquid
ANOVA	: analysis of variance
BLAIL	: Brønsted-Lewis acidic ionic liquid
BBD	: Box-Behnken design
CS	: chemical shift
FAME	: fatty acid methyl ester
IL	: ionic liquid
MIM-PS	: 3-(1-methylimidazolium -3-yl)propane-1-sulfonate
RSM	: response surface methodology
TMPO	: trimethylphosphine oxide
x_i	: coded value of the independent variable
X_i	: uncoded value of the real variable
X_0	: original value of the centered point
ΔX_i	: (variable at high level−variable at low level)/2
Y	: [%] predicted response variable
β_0	: regression coefficient
β_i	: linear terms
β_{ii}	: squared terms for the variable i
β_{ij}	: interaction terms for the interaction between variables i and j
k	: total number of variables
ε	: a random error

REFERENCES

1. K. Jacobson, R. Gopinath, L. C. Meher and A. K. Dalai, *Appl. Catal. B*, **85**, 86 (2008).
2. H. J. Kim, B. S. Kang, M. J. Kim, Y. M. Park, D. K. Kim, J. S. Lee and K. Y. Lee, *Catal. Today*, **93-95**, 315 (2004).
3. M. J. Ramos, A. Casas, L. Rodríguez, R. Romero and A. Pérez, *Appl. Catal. A*, **346**, 79 (2008).
4. X. J. Liu, H. Y. He, Y. J. Wang, S. L. Zhu and X. L. Piao, *Fuel*, **87**, 216 (2008).
5. A. Birla, B. Singh, S. N. Upadhyay and Y. C. Sharma, *Bioresour. Technol.*, **106**, 95 (2012).
6. A. Patel, V. Brahmkhatri and N. Singh, *Renew. Energy*, **51**, 227 (2013).
7. A. Casas, M. J. Ramos, J. F. Rodríguez and A. Pérez, *Fuel Process. Technol.*, **106**, 321 (2013).
8. J. A. Melero, L. F. Bautista, J. Iglesias, G. Morales and R. Sánchez-Vazquez, *Appl. Catal. B*, **145**, 197 (2014).
9. E. Raflee and S. Eavani, *J. Mol. Liq.*, **199**, 96 (2014).
10. D. M. Marinković, M. S. Stanković, A. V. Veličković, J. M. Avramović, M. R. Milandinović, O. O. Stamenković, V. B. Veljković and D. M. Jovanović, *Renew. Sust. Energ. Rev.*, **56**, 1387 (2016).
11. X. Wu, X. Han, L. Zhou and A. Li, *Indian J. Chem.*, **51A**, 791 (2012).
12. D. Kuang, S. Uchida, R. Humphry-Baker, S. M. Zakeeruddin and M. Grätzel, *Angew. Chem. Inter. Ed.*, **47**, 1923 (2008).
13. F. A. Yassin, F. Y. El Kady, H. S. Ahmed, L. K. Mohamed, S. A. Shaban and A. K. Elfadaly, *Egypt. J. Petrol.*, **24**, 103 (2015).
14. Y. Yang, W. He, C. Jia, Y. Ma, X. Zhang and B. Feng, *J. Mol. Catal. A*, **357**, 39 (2012).
15. M. Ghiaci, B. Aghabarari, S. Habibollahi and A. Gil, *Bioresour. Technol.*, **102**, 1200 (2011).
16. K. Li, Z. Yang, J. Zhao, J. Lei, X. Jia, S. H. Mushrif and Y. Yang, *Green Chem.*, **17**, 4271 (2015).
17. Z. Ullah, M. A. Bustam and Z. Man, *Renew. Energy*, **77**, 521 (2015).
18. J. Wu, Y. Gao, W. Zhang, A. Tang, Y. Tan, Y. Men and B. Tang, *Chem. Eng. Process.*, **93**, 61 (2015).
19. H. Wan, Z. Wu, W. Chen, G. Guan, Y. Cai, C. Chen, Z. Li and X. Liu, *J. Mol. Catal. A*, **398**, 127 (2015).
20. B. S. Caldas, C. S. Nunes, P. R. Souza, F. A. Rosa, J. V. Visentainer, O. de Olivera S. Júnior and E. C. Muniz, *Appl. Catal. B*, **181**, 289 (2016).
21. M. Olkiewicz, N. V. Plechkova, M. J. Earle, A. Fabregat, F. Stüber, A. Fortuny, J. Font and C. Bengoa, *Appl. Catal. B*, **181**, 738 (2016).
22. K. M. Deshmukh, Z. S. Qureshi, K. P. Dhake and B. M. Bhanage, *Catal. Commun.*, **12**, 207 (2010).
23. X. Liang and C. Qi, *Catal. Commun.*, **12**, 808 (2011).
24. K. P. Boroujeni and P. Ghasemi, *Catal. Commun.*, **37**, 50 (2013).
25. J. Li, X. Peng, M. Luo, C. J. Zhao, C. B. Gu, Y. G. Zu and Y. J. Fu, *Appl. Energy*, **115**, 438 (2014).
26. X. Chen, H. Guo, A. A. Abdeltawab, Y. Guan, S. S. Al-Deyab, G. Yu and L. Yu, *Energy Fuels*, **29**, 2998 (2015).
27. P. Gogoi, A. K. Dutta, P. Sarma and R. Borah, *Appl. Catal. A*, **492**, 133 (2015).
28. A. R. Hajipour, M. Karimzadeh and H. Tavallaei, *J. Iran. Chem. Soc.*, **12**, 987 (2015).
29. X. X. Han, H. Du, C. T. Hung, L. L. Liu, P. H. Wu, D. H. Ren, S. J. Huang and S. B. Liu, *Green Chem.*, **17**, 499 (2015).
30. E. F. Rakiewicz, A. W. Peters, R. F. Wormsbecher, K. J. Sutovich and K. T. Mueller, *J. Phys. Chem. B*, **102**, 2890 (1998).
31. Q. Zhao, W. H. Chen, S. J. Huang, Y. C. Wu, H. K. Lee and S. B. Liu, *J. Phys. Chem. B*, **106**, 4462 (2002).
32. A. Zheng, S. B. Liu and F. Deng, *Solid State Nucl. Magn. Reson.*, **55-56**, 12 (2013).
33. A. Zheng, S. J. Huang, S. B. Liu and F. Deng, *Phys. Chem. Chem. Phys.*, **13**, 14889 (2011).
34. A. Zheng, F. Deng and S. B. Liu, in *Annual Reports on NMR Spectroscopy*, G. A. Webb Ed., APNMR, UK, Academic Press, **81**, 47

(2014).
35. A. I. Khuri and J. A. Cornell, *Response surfaces: designs and analyses*, Marcel Dekker, New York, NY (1987).
36. X. Han, Y. He, C. T. Hung, L. L. Liu, S. J. Huang and S. B. Liu, *Chem. Eng. Sci.*, **104**, 64 (2013).
37. S. Liu, H. Zhou, S. Yu, C. Xie, F. Liu and Z. Song, *Chem. Eng. J.*, **174**, 396 (2011).
38. X. Han and L. Zhou, *Chem. Eng. J.*, **172**, 459 (2011).
39. X. Han, W. Yan, K. Chen, C. T. Hung, L. L. Liu, P. H. Wu, S. J. Huang and S. B. Liu, *Appl. Catal. A*, **485**, 149 (2014).
40. M. Y. Huang, X. Han, C. T. Hung, J. C. Lin, P. H. Wu, J. C. Wu and S. B. Liu, *J. Catal.*, **320**, 42 (2014).
41. S. J. Huang, C. Y. Yang, A. Zheng, N. Feng, N. Yu, P. H. Wu, Y. C. Chang, Y. C. Lin, F. Deng and S. B. Liu, *Chem. Asian J.*, **6**, 137 (2011).
42. P. Wasserscheid and W. Keim, *Angew. Chem. Inter. Ed.*, **39**, 3772 (2000).
43. X. Yan, M. Chen, Q. Dai and X. Cheng, *Chem. Eng. J.*, **146**, 266 (2009).
44. T. Singh and A. Kumar, *J. Phys. Chem. B*, **112**, 4079 (2008).